Article citation info:
Dong Y, Li T. Fault diagnosis of computer numerical control machine tools table feed system based on digital twin and machine learning. Diagnostyka. 2024;25(4):2024414. https://doi.org/10.29354/diag/195503.

DIAGNOSTYKA, 2024, Vol. 25, No. 4

e-ISSN 2449-5220
DOI: 10.29354/diag/195503

FAULT DIAGNOSIS OF COMPUTER NUMERICAL CONTROL MACHINE TOOLS TABLE FEED SYSTEM BASED ON DIGITAL TWIN AND MACHINE LEARNING

Ying DONG [1], Yanhua LI [2,*]

[1] College of Mechanical and Electrical Engineering, Shandong Vocational College of Industry, Zibo 256414, China
[2] School of Engineering Machinery, Hunan Sany Polytechnic College, Changsha 410129, China
[*] Corresponding author, e-mail: li_yanhua@163.com

Abstract

The mechanical operations performed by the computer numerical control machine tools feed system are more prone to failure, and its not conducive to the accuracy and stability of computer numerical control machine tools. As a result, this study proposes a fault diagnosis model that combines a digital twin with a multiscale parallel one-dimensional convolutional neural network. A digital twin model of the table feed system was first constructed and simulation experiments of various working conditions were conducted to obtain the missing fault data in the actual physical space. On this basis, the study utilizes the acquired signals to train the proposed migration model for diagnosis. The model extracts different types of fault features from the analog and real signals, respectively, through an intermediate multi-scale convolution algorithm. In addition, the model reduces the distributional disparities between the real and analog signals by using the Wasserstein distance as a regular term to impose constraints on the machine learning process. The study conducted simulation experiments, and the results indicated that the fault periods of the simulated and actual signals of bearing outer ring faults were 0.198s and 0.196s, respectively, with a relative error of only 1.02%. The average fault periods of the actual and simulated signals of the bearing inner ring faults were 0.199s and 0.197s, respectively, with a relative deviation of only 0.48%. In addition, the classification accuracy of the proposed model can be maintained above 95%. Thus, the proposed model has good practical value.

Keywords: digital twin, MSP-CNN, wasserstein distance, computer numerical control machine tools, table feed system, fault diagnosis

1. INTRODUCTION

Modern digital manufacturing, which primarily merges computer numerical control systems with manual machine tools, depends heavily on computer numerical control machine tools (CNCMT) [1]. The feed system in CNCMT is the direct unit involved in CNCMT cutting machining, and its stability is closely related to the productivity of the whole CNCMT [2]. During the machining process, the feed system needs to change direction and speed frequently, and often suffers from large vibration and shock, so its failure is frequent. Failure of the feed system seriously affects the efficiency, accuracy and load responsiveness of the CNCMT [3]. Therefore, in order to ensure the machining stability of CNCMT, fast and accurate Fault diagnosis (FD) of table feed system (TFS) has become an urgent problem. The conventional typical approach for the FD technique of TFS relies on manual examination, which has several drawbacks including high cost, poor diagnostic efficacy, and labor- and time-intensiveness [4]. Intelligent FD techniques have been gaining popularity recently due to the quick growth of computing technology like machine learning. Machine learning-based FD methods do not need to have a priori knowledge and have better convenience, so they are widely used in the FD of TFS. In addition, digital twin (DT) technology is newly emerging in various industries with its ability to create virtual copies of physical equipment, monitor and optimize equipment status and production processes, and improve the identification and handling of anomalies in industrial manufacturing [5]. As a result, to improve the fault detection capability of CNCMT feeding system, this research proposes a TFSFD method for CNCMT that integrates DT and machine learning. The innovations of this research are (1) to establish the DT model of CNC machining platform from two dimensions, physical space and digital space, for the common faults of CNCMT feeding system. (2) A migration diagnostic model based on multi-scale parallel 1-dimensional convolutional neural network (MSP-CNN) is constructed by making full use of the fault information in the simulated signal (S-S) as an effective supplement to the fault information in the actual signals. (3) In order to reduce the

Received 2024-04-12; Accepted 2024-11-01; Available online 2024-11-02

distributional differences between migrated fault features, the MSP-CNN is further optimized by introducing the Wasserstein distance. This research's primary contribution is the clever CNCMT feeding system that it suggests.

The study is broken up into four sections: the literature review, which covers the present status of research on the suggested technique, is the first section. The research methodology section, which mostly constructs the methodologies employed in this study, makes up the second section. The experimental validation of the suggested method is covered in the third section. The paper's outlook and summary are included in the final section.

2. RELATED WORK

The CNCMT feed system, as its core operation part, has been studied by many scholars on its FD method. Aiming at the FD problem of CNCMT machining platform feed system, Wang and other researchers proposed a new solution. To increase the effectiveness and precision of system FD, the study used CNCMT as its research object and incorporated important technologies such object-oriented knowledge acquisition, feature representation, modeling, and visualization. The suggested combination extraction technique is more precise and efficient than the conventional single extraction method, according to the experimental results [6]. To evaluate and monitor the operational status of the CNCMT, Martinova and other scholars proposed an FD method based on state detection for the TFS of the CNCMT. The method adopted a research idea based on multidisciplinary cross-fertilization and constructed a subsystem component model. The experiments proved that the proposed method can effectively detect hidden problems in the equipment [7]. To improve the machining accuracy of the machining platform, Kuo and other researchers used the Adaboost algorithm for the machining platform and proposed a new new method for chatter diagnosis based on time-varying rate sensor. Experiments proved that the method can achieve more than 98% accuracy [8]. Xia and other researchers aimed to improve the efficiency and accuracy of recognizing important wear parts in flexible manufacturing systems and proposed an acceleration sensor-based vibration detection algorithm. The proposed method utilized an artificial bee colony to optimize the initial weights of the LVQ neural network in order to improve its fault recognition effect. The method achieved fast and accurate FD of critical components in the system [9]. Deebak and Al-Turjman proposed a new FD new method based on the combination of DT and deep migration learning for the problems in CNCMT machining process. This method utilized k-type thermocouples with WiFi module on the smart tool holder to monitor the machine operating conditions in real time and obtain data in the cloud [10].

With the recent rapid development of information technology, DT technology-a method that integrates interdisciplinary linked simulation of multi-physical fields, multi-scale, and multi-probability-has been ingrained in all spheres of existence. Wang and other researchers proposed an online monitoring method based on DT architecture, which was introduced into the interconnected system to improve the real-time equipment condition monitoring. Real-time monitoring of equipment, equipment efficiency evaluation, and order scheduling were accomplished by establishing a dashboard-based operation center [11]. Ren and other researchers proposed a new management idea integrating DT and machine learning for the management of complex equipment during its life cycle, aiming to improve the responsiveness, prediction and adaptive capability of complex equipment management. The proposed method embeds a machine learning model into the DT system and uses it for the preventive maintenance of locomotive diesel engines to make the maintenance decision more intelligent [12]. Duan and other researchers took the paddle-rotor experimental platform as the research object, and established a DT technology framework system with the goal of improving its visualization monitoring and equipment monitoring capability. The system that was built made use of RS-485 and other communication protocols that enable lower-level equipment to acquire and read data in real-time. The method's efficiency was confirmed by the testing results [13]. Malek and other researchers proposed real-time DT, which is the use of intelligent maintenance system to prevent the safe operation of oil and gas, transportation and other industries effectively. This method incorporated CAE simulation to synchronize structural design-performance-inspection-maintenance. The study validated the feasibility of the LIVEDT architecture by using the LRT company and the pipeline system of the oil and gas industry as an example [14]. To automate the rotary body coating process, scholars such as Zhou and other researchers proposed a new idea of automatic monitoring and remote control of coating based on DT technology. This technology designed a remote-controlled automatic spraying production line and used multi-sensors to collect data, pre-process it, construct a unified data template and interface, and model it in 3D. The suggested strategy can successfully increase the coating spraying efficiency, according to experiments [15].

In summary, the FD method and DT technology of CNCMT feeding system gather certain scientific research achievements in their respective neighborhoods. But the current FD methods are often limited by poor intelligence, low precision, and complex operation, and there is little research on the use of DT technology in FD. As a result, this research innovation combines the two and introduces machine learning algorithms in order to realize

intelligent fault detection of the feeding system and add power to modern industrial manufacturing.

3. TFS FAULT DIAGNOSIS METHOD FOR CNCMT INCORPORATING MSP-CNN-WD AND DT TECHNIQUES

The section first constructs a DT model for TFS based on physical and digital space, and based on this, a MSP-CNN-WD machine learning model is constructed. To minimize the distributional disparities between the simulated and actual signals, the machine learning process is subject to constraints imposed by the model using the Wasserstein distance as a regular term.

3.1. DT model construction for CNC TFS based on physical and digital space

DT is an emerging interdisciplinary technology, mainly centered on modeling and data, which is of great practical significance for equipment FD [16]. The DT model of TFS constructed by DT technology enables dynamic simulation to generate scarce fault data, which can help to solve the problem of poor modeling accuracy due to few fault samples [17]. This research addresses the common faults of CNCMT feeding systems and combines the key techniques of DT to propose a FD method for CNCMT feeding systems, as shown in Figure 1. The "table" in Figure 1 is a box line representing the content of each different module. In Figure 1, this research firstly establishes the DT model of CNC machining platform from two dimensions of physical space and digital space. To address the issue of the model's low diagnostic accuracy resulting from a lack of available fault data, a large number of simulated fault signals and a small number of genuine signals are used to train and validate the constructed model.

This study constructs virtual entities in digital space from multiple perspectives, establishes mapping relationships of TFS in digital space, and generates actual data based on the actual working condition to provide sufficient training samples for building reliable FD models [18, 19]. First, the study constructs a physical model of the work feeding system to analyze the information of vibration, load, and elastic deformation generated during the motion process. The relationship between the table displacement and the servomotor rotation angle is shown in Equation (1).

$$J_0 \frac{d^2x(t)}{dt^2} + B_0 \frac{dx(t)}{dt} + K_0 x(t) = \frac{S}{2\pi} K_0 \theta_d(t) \tag{1}$$

In Equation (1), J_0 is the equivalent rotational inertia and B_0 is the equivalent damping coefficient. K_0 is the equivalent stiffness, and $x(t)$ is the displacement of the table. S is the lead of the ball screw, $\theta_d(t)$ is the rotation angle of the servo motor; t represents a time variable, used to describe physical quantities that change over time. Among them, the performance of the ball screw and the screw support greatly affects the motion accuracy of the table [20]. Therefore, in this study, in order to grasp the performance changes of the supporting bearing (SupB) and ball screw, the dynamic simulation model of the SupB and ball screw nut sub-six is constructed, as shown in Figure 2.

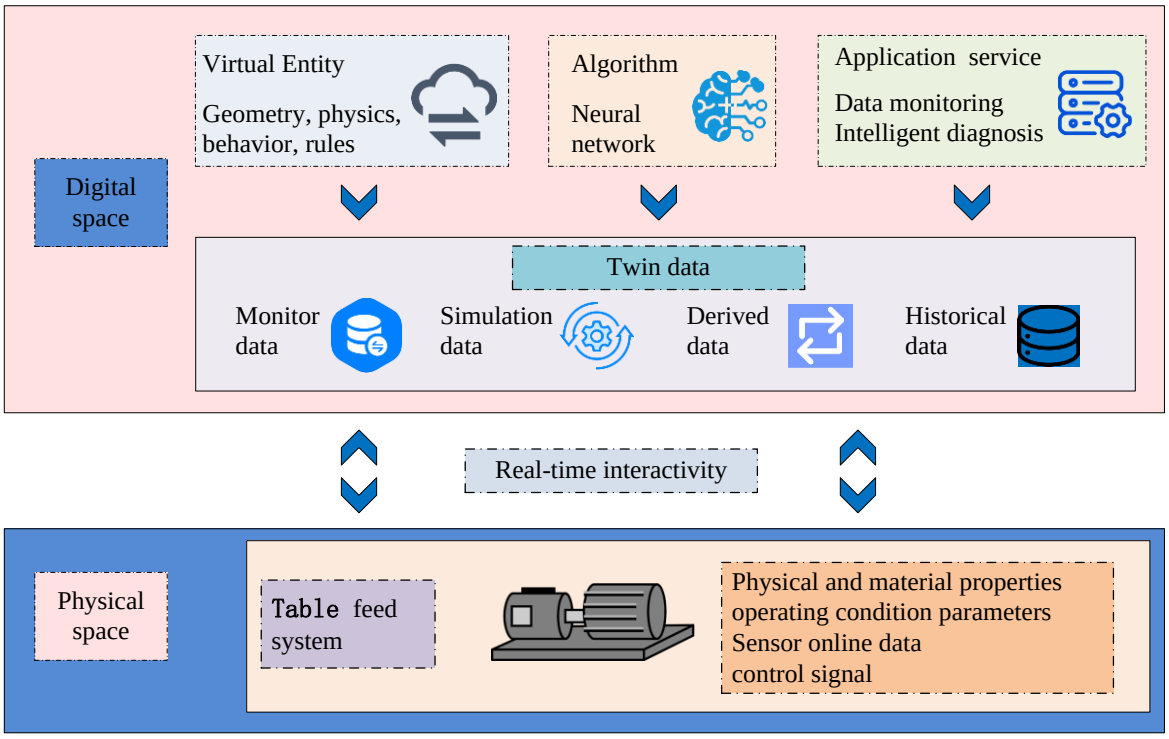

Fig. 1. Fault diagnosis scheme for table feed system based on DT technology

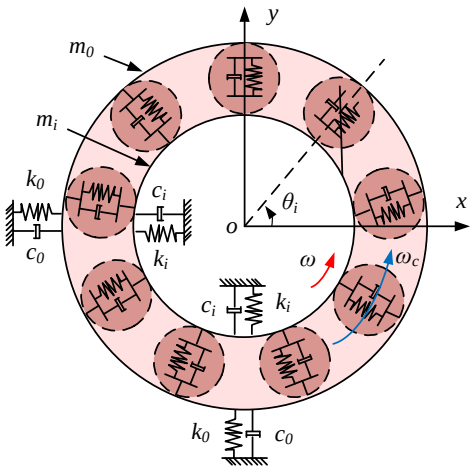

(a) Dynamic simulation model of supporting bearings

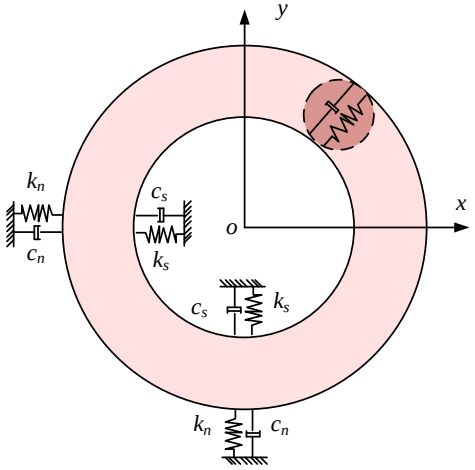

(b) Six Dynamics Simulation Model of Screw Nut Pair

Fig. 2. Dynamic simulation model of SupB and ball screw nut pair six

In Figure 2, m_i and m_o are the total mass of the inner ring (InR) and the screw, and the total mass of the outer ring (OuR) and the bearing housing, respectively. c_i and c_o are the connection damping between the screw and the fixing, and the connection damping between the bearing housing and the bed, respectively. k_i, k_0 are the equivalent connection stiffness (ECS) between the screw and the fixed place, and the ECS between the bearing housing and the bed, respectively. F_x, F_y are the components of the elastic restoring force in the x-direction and the components of the elastic restoring force in the y-direction, respectively. e is the eccentricity distance, t is the time, ω is the angular frequency of InR rotation, g is the gravitational acceleration. As a result, the differential mathematical expression for the dynamics of the SupB is shown in Equation (2).

$$\begin{cases} m_i\ddot{x}_i + c_i\dot{x}_i + k_i x_i = -F_x + em_i\omega^2\cos\omega t \\ m_i\ddot{y}_i + c_i\dot{y}_i + k_i y_i = -F_y + em_i\omega^2\sin\omega t + m_i g \\ m_o\ddot{x}_o + c_o\dot{x}_o + k_o x_o = F_x \\ m_o\ddot{y}_o + c_o\dot{y}_o + k_o y_o = F_y + m_i g \end{cases} \tag{2}$$

The mathematical expression for the elastic restoring force F in Equation (2) is shown in Equation (3).

$$F = K\delta^n \tag{3}$$

In Equation (3), K is the equivalent contact stiffness, δ is the contact deformation (CD), and n is the load deflection coefficient. Among them, δ is closely associated with the relative displacement and radial clearance of the InR and OuRs, and the CD at the i th rolling element (RolE) can be Equation (4).

$$\delta_i = (x_i - x_o)\cos\theta_i + (y_i - y_o)\sin\theta_i - c_r \tag{4}$$

In Equation (4), δ_i is the CD at the i th RolE. θ_i is the angular position of the i th RolE, and c_r is the radial clearance of the bearing. To quantify the failure situation of SupBs more clearly, two types of typical failures of the InR and OuRs of SupBs are used in this study. The expression of CD of rolling body (RB) i after the introduction of faults is shown in Equation (5).

$$\delta_i = (x_i - x_o)\sin\theta_i + (y_i - y_o)\cos\theta_i - c_r - H \tag{5}$$

The horizontal and vertical displacements of the InR of the SupB and the ball screw are represented by the letters x_i, y_i in Equation (5). The OuR of the SupB and the housing are displaced both horizontally and vertically by x_0, y_0. The depth of RB into the fault area is known as H. Figure 3(a) illustrates the change in CD between the RB and the OuR after they approach the fault area; Equation (6) provides the precise formula for this change.

$$H_o = \begin{cases} r_b - \sqrt{r_b^2 - \frac{L^2}{4}} - \left(\frac{D_o}{2} - \sqrt{\frac{D_o^2}{4} - \frac{L^2}{4}}\right) & ,8r_b h - 4h^2 \geq L^2 \\ h - \left(\frac{D_o}{2} - \sqrt{\frac{D_o^2}{4} - \frac{L^2}{4}}\right) & ,8r_b h - 4h^2 < L^2 \end{cases} \tag{6}$$

In Equation (6), D_0 is the diameter of the OuR and r_b is the radius of the RB. L is the overlapping width of the RB and the OuR, and h is the overlapping height of the RB and the OuR. The amount of change in the CD of the RB with the InR after it enters the fault region is shown in Figure 3(b), and its specific expression is shown in Equation (7).

$$H_i = \begin{cases} r_b - \sqrt{r_b^2 - \frac{L^2}{4}} + \left(\frac{D_i}{2} - \sqrt{\frac{D_i^2}{4} - \frac{L^2}{4}}\right) & ,8r_b h - 4h^2 \geq L^2 \\ h + \left(\frac{D_i}{2} - \sqrt{\frac{D_i^2}{4} - \frac{L^2}{4}}\right) & ,8r_b h - 4h^2 < L^2 \end{cases} \tag{7}$$

As a result, the simulation model of SupB failure with localized failure is constructed.

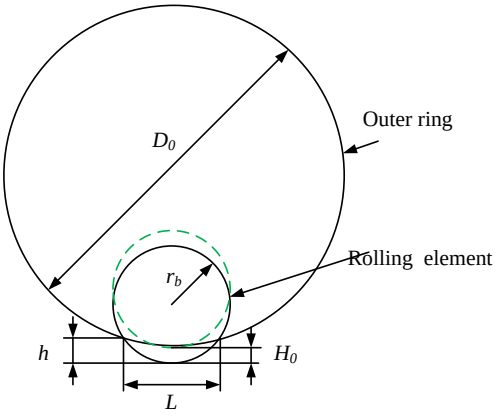

(a) The geometric relationship at the location of the outer ring fault

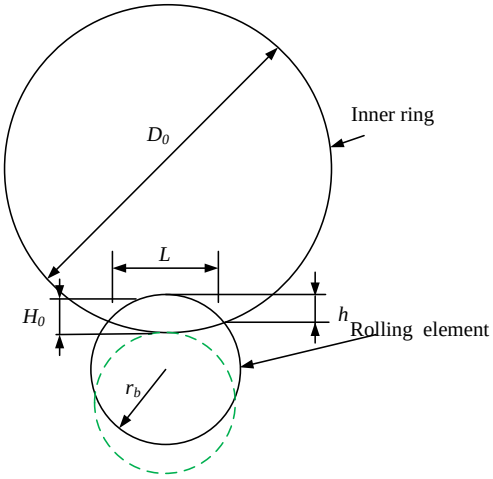

(b) The geometric relationship at the location of the inner ring fault

Fig. 3. Geometric relationship at the fault location of the inner and outer rings

The differential Equations for the dynamics of the screw nut pair established in this study are shown in Equation (8).

$$\begin{cases} m_s\ddot{x}_s + c_s\dot{x}_s + k_s x_s = P_x - e_s m_s \omega_s^2 \cos\omega_s t \\ m_s\ddot{y}_s + c_s\dot{y}_s + k_s y_s = -P_y + e_s m_s \omega_s^2 \sin\omega_s t - m_s g \\ m_s\ddot{z}_s + c_s\dot{z}_s + k_s z_s = -P_z - (T\times\tan\gamma)/r \\ m_n\ddot{x}_n + c_n\dot{x}_n + k_n x_n = -P_x \\ m_n\ddot{y}_n + c_n\dot{y}_n + k_n y_n = P_y - m_n g \\ m_n\ddot{z}_n + c_n\dot{z}_n + k_n z_n = P_z + (T\times\tan\gamma)/r - F_\mu \end{cases} \quad (8)$$

The screw mass, the screw nut's total mass, and the table are represented by the m_s and m_n in equation (8). c_s and c_n are the connection damping between the screw and the screw fixing, and the connection damping between the slider and the guideway. k_s and k_n are the ECS between the screw and the screw fixation, and the ECS between the slider and the guideway. P_x, P_y, P_z are the component of contact force in x, y, z direction. F_n is the frictional resistance between the slider and the guideway. γ is the screw lead angle, T is the motor torque, r is the radius of the screw, e_s is the eccentricity, and ω_s is the angular frequency of the screw rotation. Finally, this study used Mechanics Explorers to demonstrate the operational status of the TFS from multiple angles and in all directions, as shown in Figure 4. Figure 4 adopts a multi angle and all-round visualization approach, with each view detailing the key components of the system, including workbench, slide rail, servo motor, and base. The worktable is connected to the servo motor and ball screw through a coupling, and the rotation of the servo motor shaft is converted into the feed motion of the worktable on the guide rail using the ball screw. In the figure, sensor 1 is arranged in the z direction of the front screw support bearing seat, sensor 2 is arranged in the z direction of the guide rail end, sensor 3 is arranged in the z direction of the connection between the worktable and the screw nut, sensor 4 is arranged in the x direction of the

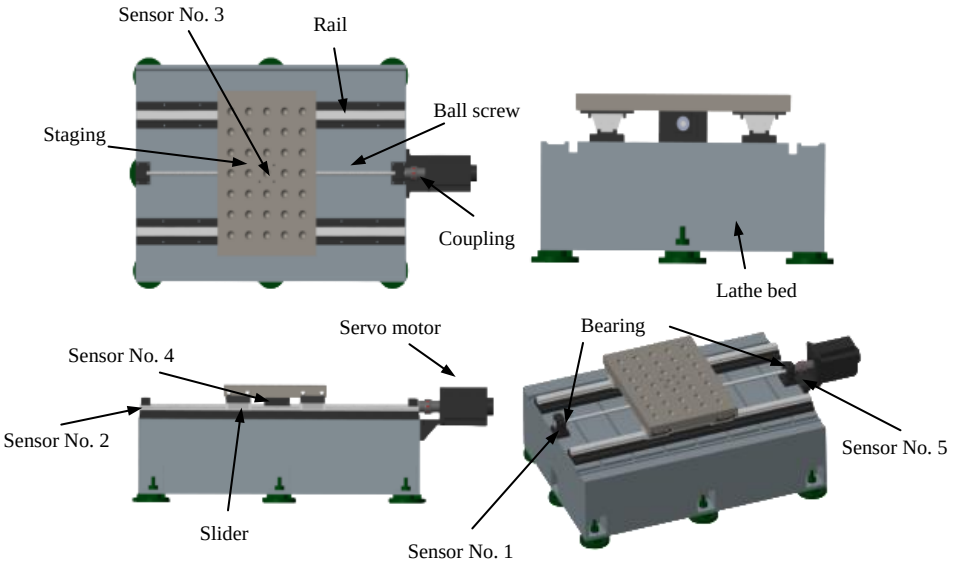

Fig. 4. Visualization of the operation status of the table feed system

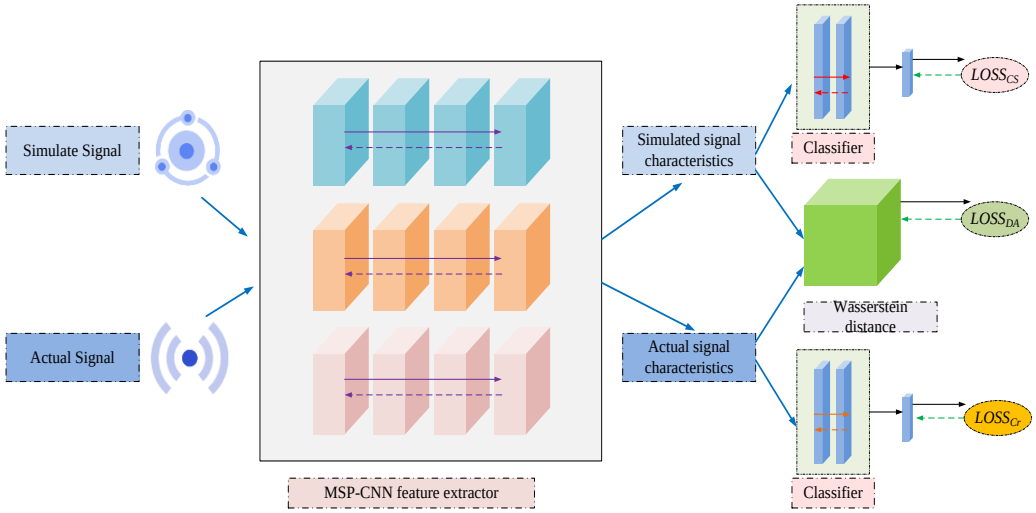

Fig. 5. Overall structure of MSP-CNN-WD model

screw nut, and sensor 5 is arranged in the z direction of the rear screw support bearing seat. The physical state of the TFS is updated in real time and visually presented when the TFS fails, based on the fault information. This achieves state synchronization between the TFS's physical entity and its virtual entity in the digital domain.

3.2. TFS fault diagnosis model based on DT technique and MSP-CNN-WD

Traditional machine learning algorithms usually require large-scale datasets for training, but massive data in real environments are difficult to obtain, making traditional machine learning algorithms likely to fall into the overfitting of a few kinds of data, which restricts the engineering applications of machine learning [21, 22]. The DT model of TFS built in this study can produce S-S with rich information on typical faults, and the signals derived from the simulation of the DT model and the real signals from sensors in engineering practice have consistent time-frequency fault characteristics [23]. In view of this, this study makes full use of the fault information in the S-S as an effective supplement to the fault information in the actual signals, and constructs a migration diagnostic model based on multi scale parallel 1-dimensional convolutional neural network (MSP-CNN). In addition, in order to reduce the distributional differences between the migrated fault features, the study further optimizes the MSP-CNN and proposes a model based on multi scale parallel 1-dimensional convolutional neural network based on Wasserstein distance (MSP-CNN-WD) model. Additionally, Figure 5 depicts the general layout of the model.

MSP-CNN is computed by performing sliding convolution on the input data in order to extract the migration fault feature extraction, which is calculated as shown in Equation (9).

$$y_{i,j}^{l+1} = f\left(\sum_{j=1}^{N}\left(x_i^l \otimes w_j^l\right)+b_j^l\right) \tag{9}$$

In Equation (9), $y_{i,j}^{l+1}$ is the corresponding value of the neuron in layer $l+1$ obtained after the convolution operation in layer l. x_i^l is the i th convolutional region in layer l. w_j^l is the j th convolution kernel of the l th layer. N is the convolution kernels. To reduce the dimensionality of the migrated fault features and to reduce the number of MSP-CNN model with training parameters, a pooling layer is added to the convolutional layer, which is calculated as shown in Equation (10).

$$P^{l+1}(i) = \max_{(i-1)W+1\le t\le iW}\left\{a^l(t)\right\} \tag{10}$$

The width of the pooling window is represented by W in Equation (10), and $P^{l+1}(i)$ is the feature vector of layer $l+1$ following the maximum pooling procedure. The MSP-CNN model needs to spend more time while pursuing high fidelity, which makes the DT model face more difficulties in synchronizing the mapping of physical entities. Consequently, the study simplifies the DT model to some extent when building it in order to reduce the complexity of the model. This results in a large distributional difference between the generated simulated and actual signals, which causes the MSP-CNN algorithm to have a large distributional difference when extracting the migrated fault features. To address this issue, this study presents the Wasserstein distance, which begins with fault feature modification and reduces distributional disparities between simulated and real signals to increase their efficacy [24,25]. Assuming that the sets of simulated and actual signals migrating fault features are P_s and P_t, the Wasserstein distance between the two signals can be Equation (11).

$$W\left(P_s,P_t\right) = \inf_{\gamma\in\Omega\left(P_s,P_t\right)} E_{(x_s,x_t)\sim\gamma}\left[\left\|x_s - x_t\right\|\right] \tag{11}$$

In Equation (11), inf is the lower bound taken, x_s is the S-S sample. x_t is the actual signal sample, and $\Omega\left(P_s,P_t\right)$ is the set of joint probability

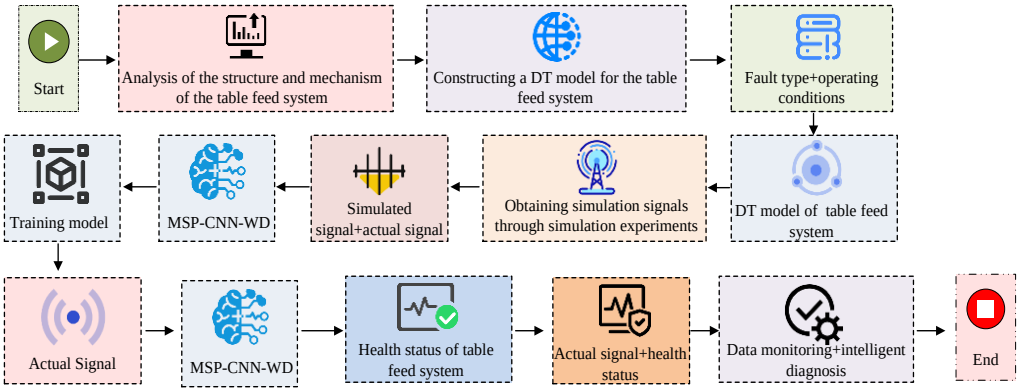

Fig. 6. Fault diagnosis process for table feed system based on DT and MSP-CNN-WD

distributions of P_s and P_t. However, the lower certainty bound cannot be solved directly by converting the Wasserstein distance into Equation (12).

$$W(P_s,P_t)=\sup_{\|f\|_L\le 1} E_{x_s\sim P_s}\left[f(x_s)\right]-E_{x_t\sim P_t}\left[f(x_t)\right] \tag{12}$$

In Equation (12), $\|f\|_L \le 1$ is 1st order Lipschitz continuous. To penalize the gradients with large values of the paradigm and increase the stability of the model, a gradient penalty function is introduced into the MSP-CNN-WD model in this study using the domain difference loss based approach. This results in the domain difference loss containing the gradient penalty function as in Equation (13).

$$\text{Loss}_{\text{DA}}=\text{Loss}_{\text{WD}}+\lambda\left(\left\|\nabla_{\hat{x}} f(\hat{x})\right\|_2-1\right)^2 \tag{13}$$

In Equation (13), λ is the gradient penalty factor. Minimizing Equation (13) enables the adaptation of the S-S to the marginal probability distribution of the actual signal migration fault features as in Equation (14).

$$\min_{\theta} Loss_{DA} \tag{14}$$

This study further optimizes the objective function of the FD model of MSP-CNN-WD as in Equation (15).

$$\text{Loss}=\min_{\theta}\left(\text{Loss}_{\text{CS}}+\alpha\,\text{Loss}_{\text{CT}}+\beta\,\text{Loss}_{\text{DA}}\right) \tag{15}$$

In Equation (15), Loss_{CS} is the cross-entropy loss for S-S classification. α is the penalty factor for cross-entropy loss of actual signal classification. Loss_{CT} is the cross-entropy loss for actual signal classification. β is the penalty factor for domain difference fitness regular term. Loss_{DA} is the domain difference loss based on Wasserstein distance.

The specific workflow of the TFS FD method based on DT and MSP-CNN-WD is shown in Figure 6. To gather the missing fault data in the real physical space, the study first built the DT model of TFS and then ran simulation tests on a range of working situations based on the model. On this basis, the study utilizes the acquired signals to train the MSP-CNN-WD migration model for diagnosis. The model extracts different types of fault features from the simulated and real signals, respectively, through an intermediate multi-scale convolutional algorithm, and restricts the learning process of the MSP-CNN by using the Wasserstein distance as a regular term to reduce the distributional difference between the simulated and real signals. The system state is then obtained by feeding the actual TFS monitoring signals into the MSP-CNN-WD model.

4. PERFORMANCE VALIDATION OF FUSED MSP-CNN-WD AND DT FAULT DIAGNOSIS METHODS

The first part of this section examines the DT acquisition and relocatability of SupB faults, with a particular emphasis on two common fault types: the screw raceway's and the screw SupB's InR and OuR faults. The FD impact of the suggested approach is then confirmed under seven CNCMT working circumstances.

4.1. Digital twin acquisition and relocatability results for support bearing failures

Due to frequent reversals, high-speed operation, and variable loads during CNC machining, the worktable feed system is prone to significant impact vibrations. Common faults such as ball screw failures, screw support bearing failures, and coupling failures are accompanied by different characteristic vibration responses. Therefore, the study deployed a contact type acceleration vibration sensor (model PCB 333B30, sensitivity of 101.6mV/g, range of ± 50gpk, frequency range of 0.5-3kHz, nonlinearity ⩽ 1%) in physical space to collect vibration signals of the worktable feed system. The layout of the sensor is shown in Figure 4 above. The first sensor is arranged in the z direction of the front screw support bearing seat, the second sensor is arranged in the z direction of the guide rail end, the third sensor is arranged in the z direction of the connection between the worktable and the screw nut, the fourth sensor is arranged in the x direction of the screw nut, and the fifth sensor is arranged in the

z direction of the rear screw support bearing seat. These sensors are accelerometers that obtain data by directly measuring vibration acceleration signals, without obtaining acceleration amplitudes through other mathematical operations. The study used LMS SCADAS Mobile equipment for signal acquisition, which has 8-channel wiring terminals, high-speed synchronous acquisition, and digital signal processing functions. The sensor is connected to LMS SCADAS Mobile, and the data is transmitted to the PC through the network and saved to the digital twin database, achieving autonomous management and monitoring of the system. The research test bench includes the basic components of the worktable feed system, simulating real working conditions, and the feed speed can be controlled by the control cabinet and computer. The sensor is connected to the LMS data acquisition device through a connecting cable. The device receives acceleration response signals under different health conditions online at a sampling rate of 6400Hz and transmits them to the computer through a network cable.

This study examines the validity of the simulation signal produced by the DT model by focusing on two common fault types: the InR and OuR faults of the screw SupB and the screw raceway. It also examines the transfer relationship between the simulation signal and the real signal in the DT from the perspectives of the probability distribution, the frequency domain, and the time domain (TiD). The screw SupB model used for the investigation is NTN6205, the TiD signal duration is 1 s, and the spectrum's frequency range is 0~100 Hz.

Figure 7 shows the TiD waveforms of the simulated and actual signals of the SupB failure. Comparing Figure 7(a) and Figure 7(c), the simulated and actual signals of the bearing OuR fault show the characteristic of "double impact", and the average fault time is 0.198s and 0.196s respectively. Compared with the two, there is only a relative error of 1.02%, and the fault period is basically the same. The amplitude of the actual and S-S of the bearing InR faults exhibit periodic changes when compared to Figures 7(b) and 7(d). Both exhibit the "double impact" features, with an average fault period of 0.199 and 0.197 seconds, respectively. Compared with the two, there is only a relative deviation of 0.48%, and the fault period is also more consistent. The average failure period is 0.199s and 0.197s respectively, with a relative deviation of 0.48%, and the failure period is more consistent.

The envelope spectrum of the real and simulated signals corresponding to the SupB's OuR and InR failures is displayed in Figure 8. From the envelope spectrum shown in Figure 8, it can be observed that the spectra of the simulated and real signals of the InR and OuR faults of the SupB contain the theoretical fault eigenfrequencies and torques, which have a more consistent intuitive effect. The result further verifies the reasonableness of the SupB OuRand InR fault modeling from the frequency domain perspective.

Figure 9 shows the distribution of the simulated TiD and real TiD signals under the failure of the OuR and InRs of the SupB. The S-S for the OuR fault of the SupB contain fewer factors and are in a simpler form, so the data distributions are more concentrated

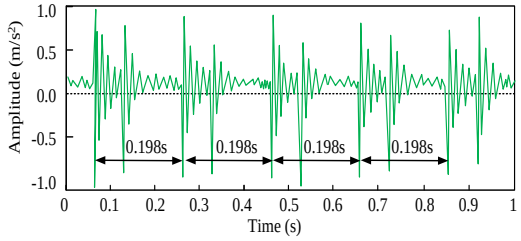

(a) Time domain waveform of outer ring fault simulation signal

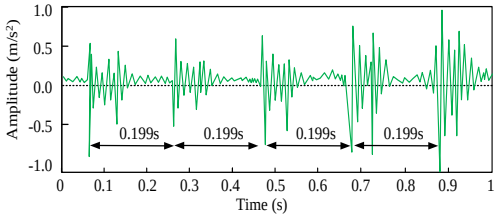

(b) Time domain waveform of inner circle fault simulation signal

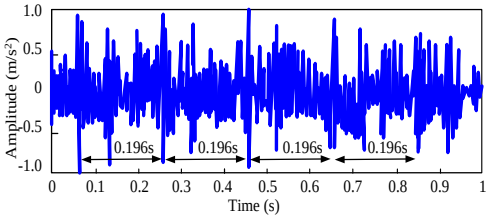

(c) Real time waveform of outer ring fault signal in time domain

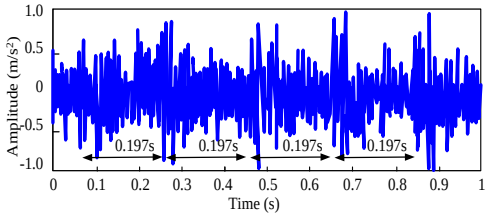

(d) Real time waveform of inner circle fault signal in time domain

Fig. 7. Simulation signal and actual signal TiD waveform of support bearing fault

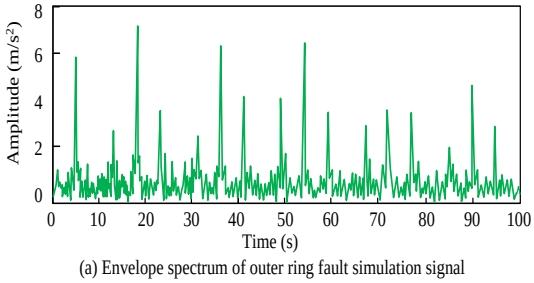

(a) Envelope spectrum of outer ring fault simulation signal

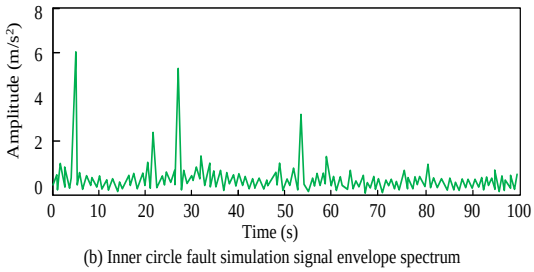

(b) Inner circle fault simulation signal envelope spectrum

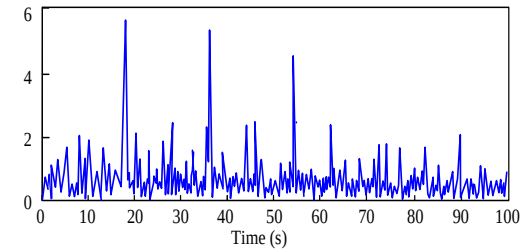

(c) Actual signal envelope spectrum of outer ring fault

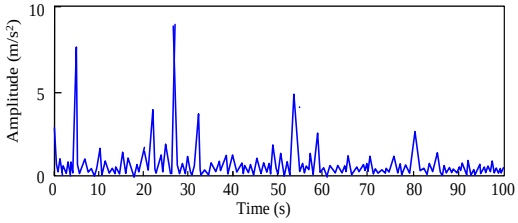

(d) Actual signal envelope spectrum of inner circle fault

Fig. 8. The envelope spectrum of the simulated signals and actual signals corresponding to the outer and inner ring faults of the supporting bearing

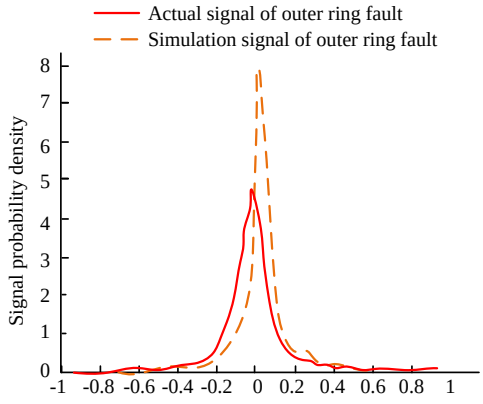

(a) Probability density curve between simulated signal and actual signal of outer ring fault

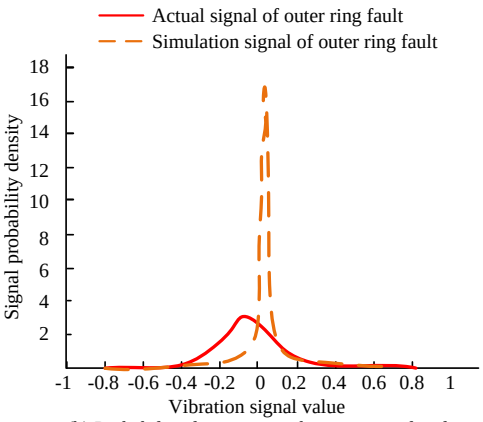

(b) Probability density curve between simulated signal and actual signal of inner ring fault

Fig. 9. Distribution of simulation and real time domain signals under outer and inner ring faults of support bearings

and show higher probability density peaks. However, in practice, the influence of a variety of random factors in other parts of the TFS makes the resulting probability density peak low and the probability distribution tends to be smooth. The probability distributions of the simulated and actual signals are very similar in the same fault case.

4.2. FD experiments and analysis of TFS

To validate the FD effect of the proposed method, seven CNCMT working conditions are set up in this study, i.e., normal condition (NC), screw raceway failure condition (LS), coupling bolt loosening failure condition (SC), guideway poor lubrication failure condition (LR), screw SupB InR failure condition (IR), screw SupB OuR failure condition (OR), and screw SupB RolE failure condition (RE). In this study, two sets of experiments are set up according to the number of samples of actual signals, corresponding to 50 and 40 samples, respectively.

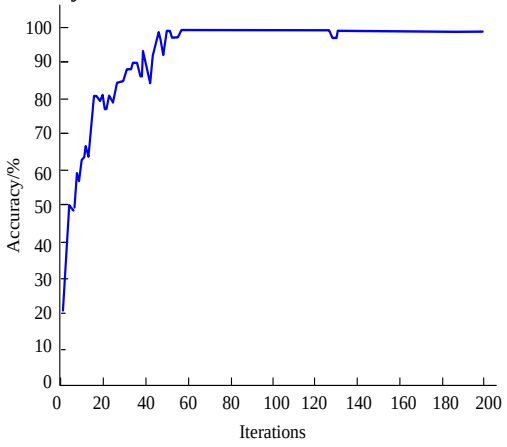

(a) Model training iteration curve

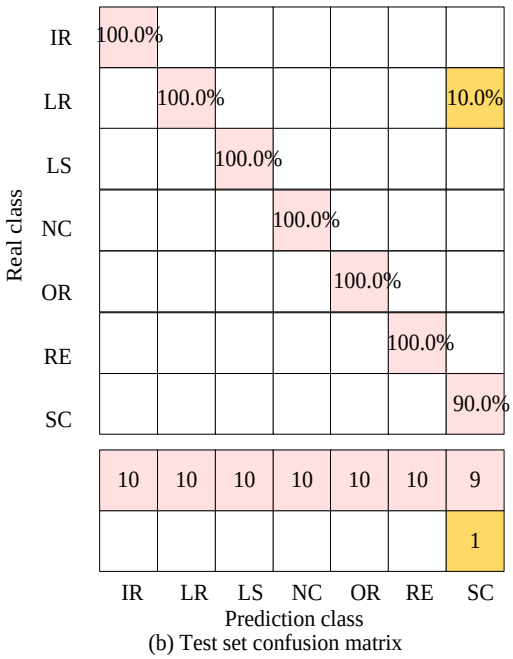

(b) Test set confusion matrix

Fig. 10. The ConM between the IC of model training and the test set when the sample size is 50

When there are 50 samples, Figure 10 displays the confusion matrix (ConM) of the test set together with the iteration curve (IC) of the model training. In the model training IC graph, the accuracy of MSP-

CNN-WD increases rapidly during 0-50 iterations during the training process, and stabilizes at around 60 iterations, and the final accuracy of the model reaches 98.61%.

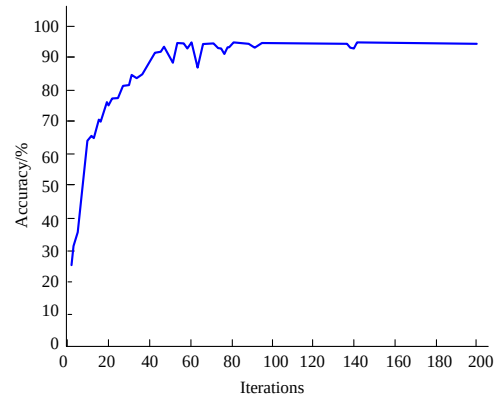

a) Model training iteration curve

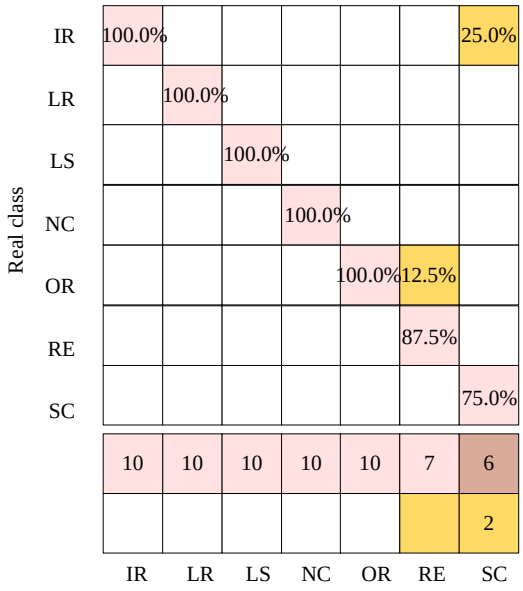

b) Test set confusion matrix

Fig. 11. The ConM between the IC of model training and the test set when the sample size is 40

When there are 40 samples, Figure 11 displays the ConM of the test set and the IC of the model training. In the model training IC graph, the accuracy of MSP-CNN-WD rises rapidly during 0-50 iterations and stabilizes at about 80 iterations, and the final accuracy of the model reaches 95.01%. Comprehensively analyzing Figure 11 and Figure 12, although the classification accuracy of the model decreases with a smaller number of samples, its accuracy can be maintained above 95%, which is able to meet the FD requirements of the actual workbench. As a result, MSP-CNN-WD has good applicability for FD of actual TFS.

The findings of MSP-CNN-WD's performance comparison with two other widely used fault detection models are displayed in Figure 12. MSP-CNN-WD has a 96.64% detection rate in Figure 12(a), compared to 93.77% for GAN and 94.23% for LSTM-GRU. Figure 12(b) shows that the missed detection rate for MSP-CNN-WD is 3.45%, compared to 16.98% and 11.97% for GAN and LSTM-GRU. As a result, MSP-CNN-WD has more superior detection fault detection performance.

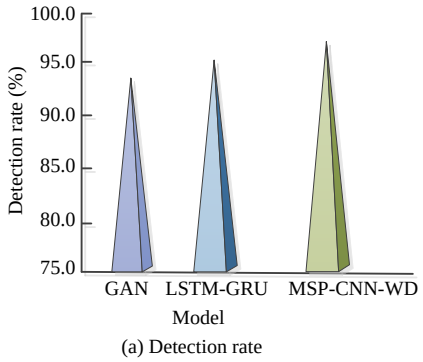

(a) Detection rate

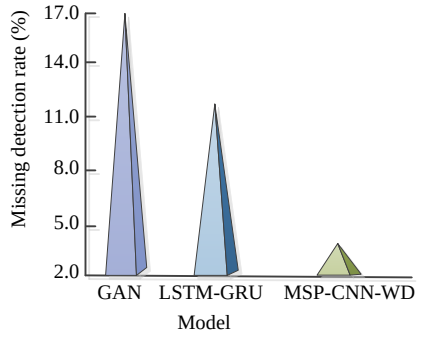

(b) Misdetection rate

Fig. 12. Comparison of fault detection performance of three models

5. CONCLUSION

The feed system of CNCMT requires frequent mechanical operations and is prone to failures, which seriously affects the efficiency, work accuracy and load responsiveness of CNCMT. Therefore, to ensure the machining stability of CNCMT, this study proposes an FD method for TFS of CNCMT by fusing DT and MSP-CNN-WD. The study conducted relevant experiments on it, and the results revealed that the average failure time of the simulated and actual signals of the bearing OuR fault is 0.198s and 0.196s, respectively, with only 1.02% relative error, and the failure period is basically the same. The average failure period of the actual and S-S of the bearing InR fault was 0.199s and 0.197s, respectively, with only a relative deviation of 0.48%. When the samples was 50, the accuracy of MSP-CNN-WD increased rapidly during 0-50 iterations, and stabilized at about 60 iterations, with an accuracy of 98.61%. When the samples was 40, the accuracy of MSP-CNN-WD stabilized at around 80 iterations, and the accuracy of the final model reached 95.01%. In Figure 12(a), the detection rate and leakage rate of MSP-CNN-WD were 96.64% and 3.45%, respectively, which were better than the comparison model. The limitation of this study was the failure to use more types of sensors to obtain

more bench information, which can be further refined in future studies.

Source of funding: *This research received no external funding.*

Author contributions: *research concept and design, Y.L.; Collection and/or assembly of data, Y.D.; Data analysis and interpretation, Y.L.; Writing the article, Y.D.; Critical revision of the article, Y.D.; Final approval of the article, Y.L.*

Declaration of competing interest: *The authors declare that they have no known competing financial interests or personal relationships that could have appeared to influence the work reported in this paper.*

REFERENCE

1. Shicong P, Guocheng W, Fuqiang T. Design and realization of CNC machine tool management system using Internet of things. Soft Computing. 2022; 26(20):10729–10739. https://doi.org/10.1007/s00500-022-06936-w.
2. Kong C, Liu W, Zhou X, Niu Q, Jiang J. A study on a general cyber machine tools monitoring system in smart factories. Proceedings of the Institution of Mechanical Engineers, Part B: Journal of Engineering Manufacture. 2021; 235(14): 2250–2261. https://doi.org/10.1177/0954405420958946.
3. Wu Y, Zhang K, Zhang Y. Digital twin networks: A survey. IEEE Internet of Things Journal. 2021;8(18): 13789–127804. https://doi.org/10.1109/JIOT.2021.3079510.
4. Zheng X, Lu J, Kiritsis D. The emergence of cognitive digital twin: vision, challenges and opportunities. International Journal of Production Research. 2022; 60(24):7610–7632. https://doi.org/10.1080/00207543.2021.2014591.
5. Zhang R, Wang F, Cai J, Wang Y, Guo H, Zheng J. Digital twin and its applications: A survey. The International Journal of Advanced Manufacturing Technology. 2022;123(11–12):4123–4136. https://doi.org/10.1007/s00170-022-10445-3.
6. Wang J, Yin W, Gao J. Cases integration system for fault diagnosis of CNC machine tools based on knowledge graph. Academic Journal of Science and Technology. 2023;5(1):273–281. https://doi.org/10.54097/ajst.v5i1.5664.
7. Martinova LI, Kozak NV, Kovalev IA, Ljubimov AB. Creation of CNC system's components for monitoring machine tool health. The International Journal of Advanced Manufacturing Technology. 2021; 117(7–8):2341–2348. https://doi.org/10.1007/s00170-021-07107-1.
8. Kuo PH, Huang MJ, Luan PC, Yau HT. Study on bandwidth analyzed adaptive boosting machine tool chatter diagnosis system. IEEE Sensors Journal. 2022;22(9):8449–8459. https://doi.org/10.1109/JSEN.2022.3163914.
9. Xia Y, Wang W, Song Z, Xie Z, Chen X, Li H. Fault diagnosis of flexible production line machining center based on PCA and ABC-LVQ. Proceedings of the Institution of Mechanical Engineers, Part B: Journal of Engineering Manufacture. 2021;235(4):594–604. https://doi.org/10.1177/0954405420970513.
10. Deebak BD, Al‐Turjman F. Digital‐twin assisted: Fault diagnosis using deep transfer learning for machining tool condition. International Journal of Intelligent Systems. 2022;37(12):10289-10316. https://doi.org/10.1002/int.22493.
11. Wang KJ, Lee YH, Angelica S. Digital twin design for real-time monitoring – a case study of die cutting machine. International Journal of Production Research. 2021;59(21):6471–6485. https://doi.org/10.1080/00207543.2020.1817999.
12. Ren Z, Wan J, Deng P. Machine-learning-driven digital twin for lifecycle management of complex equipment. IEEE Transactions on Emerging Topics in Computing. 2022;10(1):9–22. https://doi.org/10.1109/TETC.2022.3143346.
13. Duan JG, Ma TY, Zhang QL, Liu Z, Qin JY. Design and application of digital twin system for the blade-rotor test rig. Journal of Intelligent Manufacturing. 2023;34(2):753–769. https://doi.org/10.1007/s10845-021-01824-w.
14. Malek NG, Tayefeh M, Bender D, Barari A. LIVE Digital twin for smart maintenance in structural systems. IFAC-PapersOnLine. 2021;54(1):1047–1052. https://doi.org/10.1016/j.ifacol.2021.08.124.
15. Zhou K, Yang S, Guo Z, Long X, Hou J, Jin T. Design of automatic spray monitoring and tele-operation system based on digital twin technology. Proceedings of the Institution of Mechanical Engineers, Part C: Journal of Mechanical Engineering Science. 2021; 235(24):7709–7725. https://doi.org/10.1177/09544062211003617.
16. Liu W, Zhang S, Lin J, Xia Y, Wang J, Sun Y. Advancements in accuracy decline mechanisms and accuracy retention approaches of CNC machine tools: a review. The International Journal of Advanced Manufacturing Technology. 2022;121(11–12):7087–7115. https://doi.org/10.1007/s00170-022-09720-0.
17. Qiu C, Li B, Liu H, He S, Hao C. A novel method for machine tool structure condition monitoring based on knowledge graph. The International Journal of Advanced Manufacturing Technology. 2022;120(1–2): 563–82. https://doi.org/10.1007/s00170-022-08757-5.
18. Zhou L, Li F, Wang Y, Wang L, Wang G. A new empirical standby power and auxiliary power model of CNC machine tools. The International Journal of Advanced Manufacturing Technology. 2022;120(5–6):3995–4010. https://doi.org/10.1007/s00170-021-08274-x.
19. Fernandes M, Corchado JM, Marreiros G. Machine learning techniques applied to mechanical fault diagnosis and fault prognosis in the context of real industrial manufacturing use-cases: a systematic literature review. Applied Intelligence. 2022;52(12): 14246–14280. https://doi.org/10.1007/s10489-022-03344-3.
20. Guo M, Fang X, Hu Z, Li Q. Design and research of digital twin machine tool simulation and monitoring system. The International Journal of Advanced Manufacturing Technology. 2023;124(11–12):4253–4268. https://doi.org/10.1007/s00170-022-09613-2.
21. Hou Z, Yu Z. Two‐layer model of equipment fault propagation in manufacturing system. Quality and Reliability Engineering International. 2021;37(2):743-762. https://doi.org/10.1002/qre.2761.
22. Kenett RS, Bortman J. The digital twin in Industry 4.0: A wide‐angle perspective. Quality and Reliability

Engineering International. 2022;38(3):1357-1366. https://doi.org/10.1002/qre.2948.
23. Xiong M, Wang H, Fu Q, Xu Y. Digital twin–driven aero-engine intelligent predictive maintenance. The International Journal of Advanced Manufacturing Technology. 2021;114(11–12): 3751–3761. https://doi.org/10.1007/s00170-021-06976-w.
24. Choudhuri S, Adeniye S, Sen A. Distribution alignment using complement entropy objective and adaptive consensus-based label refinement for partial domain adaptation. Artificial Intelligence and Applications. 2023;1(1):43–51. https://doi.org/10.47852/bonviewAIA2202524.
25. Bhosle K, Musande V. Evaluation of deep learning CNN model for recognition of devanagari digit. Artificial Intelligence and Applications. 2023;1(2): 114–118. https://doi.org/10.47852/bonviewAIA3202441.

Dong YING
February 1987, female, the Han nationality, Chengwu County, Shandong Province, graduated from Shandong University of Science and Technology in 2009 with a bachelor's degree in Mechanical Design, Manufacturing, and Automation, and graduated from Shandong University with a master's degree inMechanical Manufacturing and Automation in 2014. Now she is a teacher of College of Mechanical and Electrical Engineering, Shandong Vocational College of Industry.Her main research interests are CNC machining technology, intelligent manufacturing technology, fault diagnosis research, intelligent welding technology, etc.
Work experience: From September 2014 to June 2016, she worked at AVIC Shenyang Aircraft Industry (Group) Co., Ltd. as a technician; from August 2016 to present, she has worked at the College of Mechanical and Electrical Engineering of Shandong Vocational College of Industry as a teacher.
Academic situation: She has published 6 academic papers, participated in the compilation of the 14th Five-Year National Planning Textbook "Basics of Mechanical Design", participated in 3 scientific research projects, and published 3 computer software copyrights. She won the second prize in the 2019 National Vocational School Skills Competition Teaching Ability Competition; the third prize in the 2021 National Vocational School Skills Competition Teaching Ability Competition; the third prize in the 2022 National Vocational School Skills Competition Teaching Ability Competition. She won the first prize in the 2022 Shandong Province Ninth College Young Teachers Teaching Competition.
e-mail: dongy0221@163.com

Yanhua LI
Obtained her Bachelor's degree in Equipment and Engineering Management from Chang'an University in 2001. Currently, she works as an associate professor at the Engineering Machinery College of Hunan Sany Polytechnic College. Her research areas include construction machinery technology, numerical control machine tools, and Hydraulic Transmission Technology.
From 2001 to 2009, served as a Design Engineer at the Road Machinery Research Institute of XCMG, engaged in the development and design of road roller products.
From 2009 to 019, worked as a Design Supervisor at the Research Institute of Hunan Zhongda Chuangyuan CNC Equipment Co., Ltd., responsible for the design and development of CNC bevel gear grinding machines, milling machines, and cylindrical bevel gear grinding machines.
From 2019 to present, employed as a Professional Teacher at Hunan Sany Polytechnic College, teaching core courses such as Engineering Machinery Product Service Technology.
Published 6 academic papers. Authored 1 academic book/textbook. Participated in a total of 5 research projects. Held 10 patents. Obtained 4 software copyrights.
e-mail: li_yanhua@163.com